

How to Optimize Multispecies Set Predictions in Presence–Absence Modeling ?

Sébastien Gigot–Léandri^{1,2} | Gaétan Morand² | Alexis Joly¹ | François Munoz⁴
 David Mouillot² | Christophe Botella¹ | Maximilien Servajean^{1,3}

¹UMR LIRMM, University of Montpellier, Inria, CNRS, France

²UMR Marbec, University of Montpellier, IRD, CNRS, Ifremer

³University of Montpellier Paul Valéry, Montpellier, France

⁴Laboratoire de Biométrie et de Biologie Evolutive, Université Lyon 1, Villeurbanne, France

Author Contributions

SGL conceived and designed the study, developed the MaxExp optimization framework, implemented all core algorithms, and led the analyses. GM developed and implemented the modeling pipeline for the Reef Life Survey case study. AJ, MS, CB, and FM contributed to the study design, methodological refinements, and interpretation. FM and DM provided ecological expertise and guidance on the ecological relevance of model evaluation and species assemblage predictions. SGL wrote the first draft of the manuscript, and all authors contributed to manuscript revision.

Data Availability Statement

All results and graphs in this study are reproducible via the available code and the ready to download model outputs and ground truth data :

Code : Github: https://github.com/sebastiengl/score_maximisation

Model outputs / Ground truth: Seafile : <https://lab.plantnet.org/seafile/d/822f01a64a614759b11b/>

The related studies and data supporting the findings of this paper are also openly available :

Case Study 1 : Paper: [Picek et al., 2024](#) | Challenge & Model: <https://www.kaggle.com/code/picekl/sentinel-landsat-bioclim-baseline-0-31626>

Case Study 2 : Paper: [Morand and Mouillot, 2025](#) | RLS: [Edgar and Stuart-Smith, 2014](#)

Case Study 3 : Paper: [Zipkin et al., 2023](#) | BBS: [Hudson et al., 2017](#) | eBird: [Sullivan et al., 2014](#) | Modified Model : https://github.com/sebastiengl/CS3_modified_model

Keywords

species distribution models, presence-absence predictions, binarization methods

Number of words in Abstract: 146

Number of words in Main Text: 4165

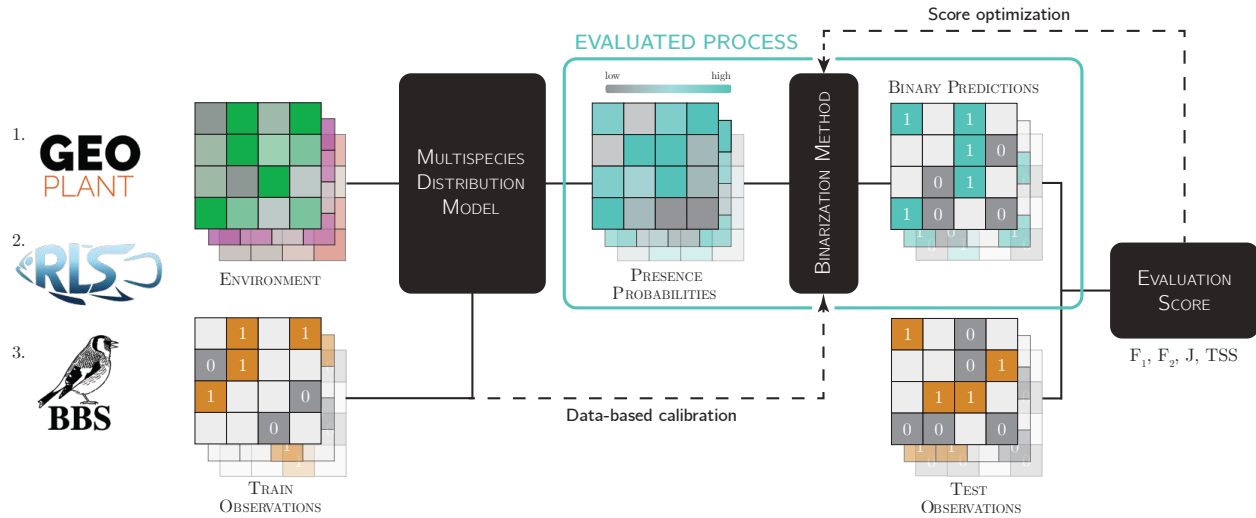
Number of References: 37

Number of Figures & Tables: 6

Sébastien Gigot–Léandri

E-mail: s.gigotleandri@lirmm.fr

Tel: +33 6 75 00 89 93



Across three case studies, we evaluate newly developed unsupervised binarization methods against established calibration-based approaches. MaxExp, the framework introduced here, combines score maximization with the advantages of unsupervised optimization and delivers improved multispecies predictions across ecosystems.

1 Abstract

Species distribution models (SDMs) commonly produce probabilistic occurrence predictions that must be converted into binary presence–absence maps for ecological inference and conservation planning. However, this binarization step is typically heuristic and can substantially distort estimates of species prevalence and community composition. We present MaxExp, a decision-driven binarization framework that selects the most probable species assemblage by directly maximizing a chosen evaluation metric. MaxExp requires no calibration data and is flexible across several scores. We also introduce the Set Size Expectation (SSE) method, a computationally efficient alternative that predicts assemblages based on expected species richness. Using three case studies spanning diverse taxa, species counts, and performance metrics, we show that MaxExp consistently matches or surpasses widely used thresholding and calibration methods, especially under strong class imbalance and high rarity. SSE offers a simpler yet competitive option. Together, these methods provide robust, reproducible tools for multispecies SDM binarization.

2 Introduction

Biodiversity is declining globally, so urgent conservation and management strategies require a deeper understanding of the intricate species dynamics across space and time (Dirzo et al., 2014). In this context, Species Distribution Models (SDMs) are crucial tools for biodiversity monitoring and ecological assessment, as they can help understand species ecological niches, and predict species habitat suitability (Guisan et al., 2013, Guisan and Thuiller, 2005). Modern SDMs, like JSDM (Wilkinson et al., 2021), DeepSDM (Deneu et al., 2021) or site occupancy models (Chambert et al., 2015) address complex multispecies prediction tasks depending on diverse covariates, producing either suitability indices or, when calibrated with presence-absence data, presence probability estimates. Many practical ecological applications however still require binary decisions—namely, determining whether a species (or a set of species) should be present or absent at a given site (Araújo et al., 2006, Luoto et al., 2006, Jiménez-Valverde and Lobo, 2007). Such decisions are critical for achieving various objectives, including estimating species ranges (Hellegers et al., 2025), predicting species assemblages (Guisan and Rahbek, 2011), mapping potential distributions of protected species (Zizka et al., 2020), or forecasting species richness under scenarios of environmental changes (Guisan and Rahbek, 2011). Thus, even with accurate presence probability estimates, binarizing the model outputs is necessary. Many widely used evaluation scores in ecology—such as F_1 -score, the Jaccard index, or the True Skill Statistic (TSS)—are based on binary predictions and set values (i.e., the number of True Positives, True Negatives, False Positives, False Negatives). These scores evaluate the agreement between predicted and observed presence/absence patterns, thereby assessing the combined efficiency of prediction and binarization steps (see Figure 1). However, this step introduces uncertainty and biases due to the information loss and arbitrary decisions inherent to thresholding (Nenzén and Araújo, 2011).

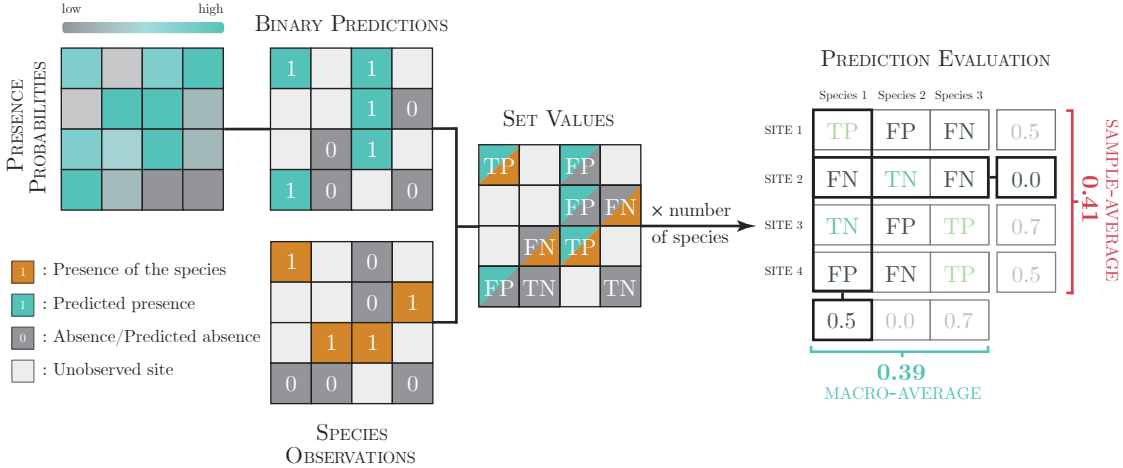
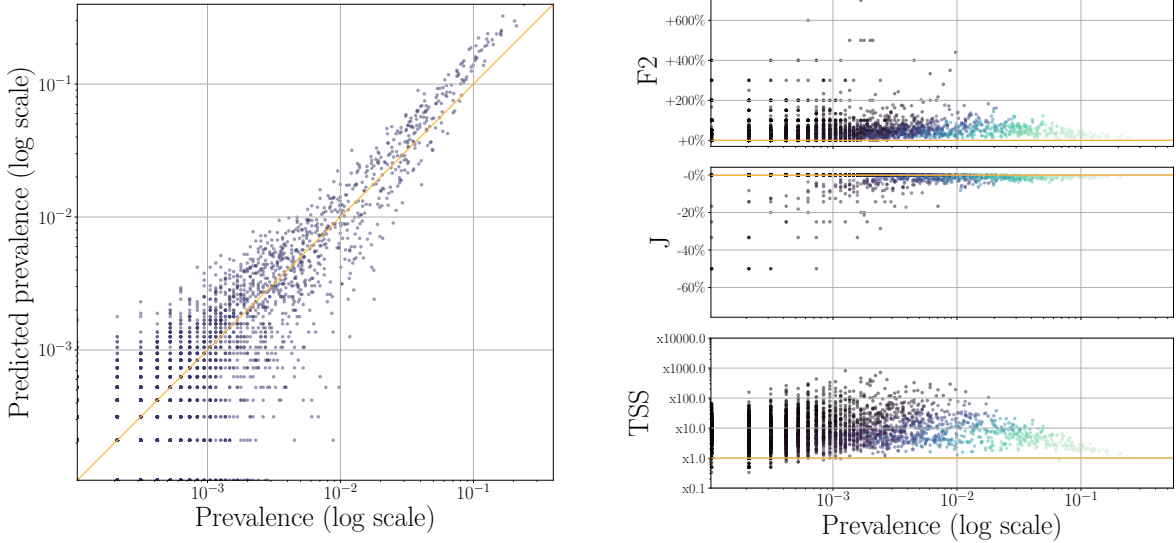


Figure 1: Evaluation pipeline of species presence/absence predictions. The spatial probability estimates (in blue shade) outputs by the model for a given species are converted into binary presence/absence predictions (blue/grey squares) where observations have been made. The results are then compared to the observed occurrence data (orange for presence, grey for absence). From this comparison, we get set values for each species at each site considered (TP: True Positive, TN: True Negative, FP: False Positive and FN: False Negative). The prediction score can be then calculated in 2 main ways: macro-averaging, i.e., the mean of scores calculated individually for each species (blue), or the sample-averaging, calculating the mean of species scores computed at each site (red).

In practice, one must select one or several evaluation scores, and this choice has important consequences for the resulting species predictions of a selected SDM. Each score is sensitive to different types of error: For instance, some are more lenient towards false positives, while others are more conservative on occurrence prediction. As such, maximizing different scores can lead to broadly different predictions. For instance, Figure 2 depicts the influence of score choice on predicted prevalence (the proportion of sites where the species is predicted present). Therefore a score may be chosen to meet a specific study objective, such as predicting the species composition at a given site while minimizing the chance of missing rare species, or constructing a unbiased map of species richness. In the same manner, binary decisions must then be taken in accordance with that objective.



(a) Species prevalences of the sample-average F_1 -optimized predictions (y-axis) compared to true species prevalence (x-axis). Log-scale is used to underline how prevalence error has much higher variance for rare species.

(b) Change in predicted prevalences for different scores. To reduce displayed impact from prediction variance error, the results are this time compared directly to the prevalence predicted with F_1 -score via their ratio (y-axis), in function of true prevalence (x-axis). The color gradient follows the predicted prevalence under F_1 -score.

Figure 2: Study of the predicted species prevalence maximizing sample-average scores for the GeoPlant 2024 data (See Case 1 for more details of the model and dataset). Log values of predicted and true number of occupied sites + 1 are shown. The choice of evaluation score markedly influences predictive outcomes: the F_1 -score produces balanced results with strong correlation to prevalence ($R_2 : 0.69$, $R_2 : 0.82$ in log-log scale). The F_2 -score over-predicts the number of occupied sites, particularly for rare species. The Jaccard index yields the opposite effect with smaller magnitude, with rare species predicted in $\sim 20\%$ less sites. The TSS generates a more complex over-prediction pattern, with a curve-shaped ratio centered around a factor 10.

Therefore, identifying a general binarization method that performs well across a diverse range of scores remains both a critical and major challenge. Although the thresholding problem has often been addressed in the literature, most of the studies considered approaches relying on additional observation data (Petitpierre et al., 2017, Li and Guo, 2013, Zurell et al., 2020), which entail increased risks of overfitting calibration (Chollet Ramampiandra et al., 2023, Randin et al., 2006), and substantial computational burden — particularly as the number of species increases. For rare species, allocating a significant portion of the already limited presence data to threshold calibration can further increase prediction uncertainties. (Nenzén and Araújo, 2011) noted that the SDM binarization step is one of the least explored source of error for these models whereas there are potentially many applicable rules for this binarization, and, as a consequence, the binarization method is often chosen arbitrarily.

The present study introduces a generic framework that optimizes the binarization process for multiple species by maximizing the expected of the provided evaluation score. In contrast to supervised thresholding methods, our method does not require more data than the data used to train the model, is applicable to a wide range of SDM evaluation scores, and achieves equivalent or superior performance compared to state-of-the-art methods across three distinct case studies and modeling approaches evaluated with 4 different sample-average scores. This demonstrates both the robustness and practical relevance of our new method for a myriad of ecological applications where binary presence-absence model outputs underpin conservation and management decisions.

3 Materials & Methods

This study addresses the optimization of presence-absence multispecies predictions using sample-averaged (or horizontal) scores—that is, scores calculated for each site across all species and then averaged over all sites to produce a global performance measure. This approach contrasts with the more conventional use of macro-averaged (or vertical) scores, where scores are computed separately for each species and then averaged across species (Figure 1). In both frameworks, the optimization targets the agreement between predicted and observed species compositions (e.g. through F_1 -score). The horizontal perspective (sample-average), however, emphasizes the accuracy of predicted species assemblages at site level, whereas the vertical perspective (macro-average) emphasizes the accuracy of species prevalence across the sites. By focusing on per-site assemblages and sample-averaged scores, our approach addresses an underexplored area in the literature with the potential to provide more accurate and realistic species assemblage predictions. Noticeably, the introduced framework is transferable to optimize SDM-binarization based on vertical scores as well.

3.1 Problem formulation

In the context of multispecies distribution models, a prediction is made at each site, and a local score can be calculated using a given evaluation score. The final score is then computed as the mean of local scores across sites. We define the problem of species assemblage prediction in a given sampled site as a solvable optimization problem. This sample site is linked to an input environment $x \in \mathcal{X}$. Let us denote $y \in \mathcal{Y}$ the species assemblage associated to this input environment x , with $\mathcal{Y} = \mathcal{P}(\{1, \dots, N\})$ being the set of all possible species assemblages - i.e. the set of subsets of $1, \dots, N$. The assemblage y is supposed to be sampled from a probability measure $\mathbb{P}_{X=x}(Y)$.

Now, let $U : \mathcal{Y} \times \mathcal{Y} \rightarrow \mathbb{R}$ be a similarity function measuring how close two assemblages are (e.g. F_1 -score, Jaccard or TSS). This function must satisfy the following assumption:

A1 : U only depends on the number of true positives (TP), false positives (FP), true negatives (TN) and false negatives (FN). It increases with TP and TN, but decreases with FN and FP. This assumption is verified by most of the popular metrics in the literature.

We will also consider a second assumption as:

A2 : the presences of all species are considered independent events from each other.

Our goal is to find the optimal species set y^* maximizing the expected agreement between the prediction y' and the species assemblage y in regard to U , which is defined as:

$$y^* = \arg \max_{y' \in \mathcal{Y}} \mathbb{E}_{Y|X=x}[U(Y, y')] = \arg \max_{y' \in \mathcal{Y}} \sum_{y \in \mathcal{Y}} \mathbb{P}_{X=x}(Y = y) U(y', y). \quad (1)$$

The core challenge stems from the cardinality of \mathcal{Y} , which grows exponentially with the number of species N . Since \mathcal{Y} is iterated over twice (for both y' and y , representing the predicted and true species sets, respectively), the problem becomes computationally intractable with a total complexity of $\mathcal{O}(2^N)$. The objective of the present framework is to address this issue under some assumptions to render the problem computationally solvable. A similar strategy was used in (Nan et al., 2012), but their approach was limited to F_β measures and was not designed in a context of ecological application.

Solving the optimization problem under the additional assumptions that the prediction returns k species and that species are independent under **A2** becomes trivial. To see this, consider an assemblage of size n species. We have the following relations :

$$FP = k - TP \quad FN = n - TP \quad TN = N - k - n + TP \quad (2)$$

In other words, all quantities depend on TP. Hence, considering assumptions **A1** and **A2** together, maximizing U leads to the selection of the k most probable species. Since this strategy is optimal for any size n , it is globally optimal. Had the species not been independent, the k most likely species could potentially depend on the set size n . Hence, the expected score $\mathbb{E}_{Y|X=x}[U(Y, .)]$ is maximized by the topk predictor. The overall problem can therefore be rephrased as finding the optimal number k of species per site to predict.

3.2 MaxExp framework

Given **A1**, the similarity function can be reformulated as depending on the different set values:

$$U(y, y') = U'(|y \cap y'|, |y'| - |y \cap y'|, |y| - |y \cap y'|, N - |y \cup y'|) = U'(TP, FP, FN, TN). \quad (3)$$

Moreover, let us denote $\pi_x : \{1, \dots, n\} \rightarrow \{1, \dots, n\}$ a permutation of species index in decreasing order of marginal probability $(\mathbb{P}_{X=x}(Y_i = 1))_{i \leq n}$. Considering an observation (x, y) and $k = |y'|$, the parameter to optimize, let us define the following statistics:

$$S_k = \sum_{i=1}^k y_{\pi_x(i)}, \quad S^k = \sum_{i=k+1}^N y_{\pi_x(i)}. \quad (4)$$

Given **A2**, S_k and S^k are independent. Since FP and TN can be derived from TP and FN, and since $TP = S_k$ and $FN = S^k$, we can reformulate the optimization problem as finding:

$$k^* = \arg \max_{k \in \mathbb{N}} \sum_{k_1} \sum_{k_2} \mathbb{P}_{X=x}(S_k = k_1) \mathbb{P}_{X=x}(S^k = k_2) U'(k_1, k - k_1, k_2, N - k - k_2) \quad (5)$$

Solving this problem can be achieved in $\mathcal{O}(N^3)$, given that the $2N^2$ values describing the distribution of S_k and S^k for any k can be computed with a complexity equal or less than $\mathcal{O}(N^3)$. Given **A2**, consider the following relations :

$$\mathbb{P}_x(S_{k+1} = k_1) = \mathbb{P}_x(Y_{k+1} = 1) \mathbb{P}_x(S_k = k_1 - 1) + (1 - \mathbb{P}_x(Y_{k+1} = 1)) \mathbb{P}_x(S_k = k_1) \quad (6)$$

$$\mathbb{P}_x(S^{k-1} = k_2) = \mathbb{P}_x(Y_k = 1) \mathbb{P}_x(S^k = k_2 - 1) + (1 - \mathbb{P}_x(Y_k = 1)) \mathbb{P}_x(S^k = k_2) \quad (7)$$

where we denote $\mathbb{P}_{X=x}$ as \mathbb{P}_x for readability reasons. With the probabilities now expressed recursively, computing them does not increase the overall complexity of the maximization procedure. In particular, we adopt the plug-in rule strategy where $\mathbb{P}_x(Y_k)$ is replaced by an estimator of the marginal conditional probability of presence, $\hat{\eta} : \mathcal{X} \rightarrow [0, 1]^N$. This conditional probability is typically the output of a SDM or a site occupancy model.

In summary, under assumptions **A1** and **A2**, it is possible to maximize the expected similarity score in $\mathcal{O}(N^3)$ given some estimated marginal conditional probabilities. Reduction to quadratic complexity is even possible for some scores, like the F_1 -score or the Jaccard index with a trick explored for F_β -measures in (2012).

Also, given a similarity function satisfying **A1**, we proved that MaxExp yields the best theoretical predictions given some true conditional probability as long as they satisfy **A2**. An example of MaxExp implementation can be found in Section A of the Supplementary Material. In the following sections, a comparative analysis is conducted to assess the framework's performance in concrete scenarios compared to different reference methods.

3.3 Reference binarization methods

To assess the performance of our MaxExp framework, we performed a comparison against a set of reference binarization methods detailed in Table 1. These baselines include both established approaches from the literature on species presence-absence predictions (e.g., methods (1), (2), and (3) [Nenzén and Araújo, 2011](#)) and conceptually distinct strategies that we constructed for this study, such as thresholding presence-only predictions (method (4) [Dorm et al., 2024](#)) and from conformal prediction (method (5) [Angelopoulos and Bates, 2022](#)). Naturally, our framework does not need any calibration, the only potential use of a validation set would have been for the calibration of the predictive model itself. To assess models' ability to estimate presence probabilities, calibration curves on training and testing data are available in Supplementary Material (Section D).

Several studied methods however require to calibrate some parameters, and a calibration set has to be constructed to optimize these parameters according to any score used before

predictions. Two distinct experiments have thus been run: original test data have been split in a 0.2/0.8 uniformly distributed, where the first part constitutes a validation set and the second the actual data used for score evaluation. A first test has been made in each study with a calibration of these methods using the train set and the output of the model on the latter. In this case, the calibration only reuses the information from which the model has been trained and does not require additional data. A second one has been carried out, taking this time the validation set for calibration. In the last case, this calibration can be seen as an additional source of information which these supervised methods will benefit from.

Reference methods	Principles
(1) Top K	A naive, constant baseline that returns the K most probable species predicted, with K optimized globally for all sites in the validation set.
(2) Threshold $t_{0.5}$	Assumes that the predicted probabilities are centered around the decision boundary, meaning that on average, presences have predicted probabilities above 0.5 and absences below 0.5.
(3) Globally optimized threshold t	Use a single threshold shared across species, selected by testing candidate values between 0 and 1 in increments of 0.01.
(4) Species frequency threshold t_f	Compute the empirical frequency f_i of each species and return the f_i^{th} highest percentiles of predicted probabilities. Adjusts thresholds per species according to observed prevalence, better capturing rare versus common species, but assumes that past frequencies reflect the underlying probability distribution.
(5) Optimized recall R_{opti}	Minimize the number of presences predicted while enforcing a lower bound on empirical recall. The recall bound itself is chosen from candidate values between 0 and 1, evaluated in increments of 0.01, to maximize the chosen score.
(6) Set Size Expectation (or SSE)	Return the S most probable species, where S is the estimated species richness, obtained by rounding the sum of predicted probabilities across species.

Table 1: Summary of the different reference methods studied.

In the following, we refer to supervised methods as those requiring the optimization or calibration of one or more parameters. This category includes methods (1), (3), (4) and (5). Methods that do not require parameter optimization or calibration—including our MaxExp framework—are referred to as unsupervised.

3.4 Evaluation scores

As mentioned earlier, our MaxExp framework can be applied to any target score that satisfies assumptions **A1** and **A2**. In our experimental analysis, we focused on the following four evaluation scores, commonly used in ecology: : F_1 , F_2 , the Jaccard index J , and the True

Skill Statistic TSS .

F_β -score (F_β)

$$F_\beta = \frac{(1 + \beta^2)TP}{(1 + \beta^2)TP + \beta^2FN + FP} \quad (8)$$

The F_β -score defines a parametrized score, with β adjusting the weight of the recall and so the weight of false negatives. The F_1 -score, corresponding to the unweighted mean, is widely used in ecology (Legendre and Legendre, 2012 Li and Guo, 2013 Hellegers et al., 2025). The F_2 -score, more rarely employed, accentuates the weight of false negatives and consequently favors predictions with an increased number of positives predicted, as seen in Figure 2. In ecological applications where false negatives are more costly than false positives, this score reflects well the intended behavior for the predictions.

Jaccard Index (J)

$$J = \frac{TP}{TP + FN + FP} \quad (9)$$

The Jaccard index is commonly used in ecological studies — from community comparisons (Legendre and Legendre, 2012) to fragmentation analyses (Laurance et al., 2007) — and in classification tasks.

True Skill Statistic (TSS)

$$TSS = \frac{TP}{TP + FN} + \frac{TN}{TN + FP} - 1 \quad (10)$$

Popularized by Allouche et al., 2006 for its perceived independence from species prevalence (later refuted by Leroy et al., 2018)), the TSS is still widely used in ecological modeling. Contrary to F_β and J , TSS evaluates TN and is consequently sensitive to the double-zero problem (Legendre and Legendre, 2012), which limits its ecological interpretability and explains its particular behavior with unbalanced classes (Figure 2).

4 Applications

The analysis of our MaxExp framework is conducted for three case studies, each evaluated across multiple decision functions and performance metrics. These case studies were selected to maximize the diversity of testing conditions, thereby assessing both the robustness and flexibility of the proposed framework. The three case studies span distinct taxonomic groups, employ different modeling techniques, and vary by several orders of magnitude in both the number of species and sites. Each study builds upon previous work (Picek et al., 2024,

Morand and Mouillot, 2025 and [Zipkin et al., 2023](#)), and only the key methodological aspects are presented here. For further details on the data and modeling processes, please refer to the respective original studies.

4.1 Case study 1: GeoPlant 2024

The first case study is derived from the GeoLifeCLEF 2024 challenge, a yearly machine learning challenge focused on the European plant species from the GeoPlant 2024 dataset [Picek et al., 2024](#). The training data comprises presence-absence (PA) surveys, totaling approximately 90,000 samples and covering 5,016 species of the European flora for presence-absence observations. The input predictors used for species prediction fall into three main categories:

- Satellite image patches: 3-band (RGB) and 1-band (NIR) images with 128×128 pixel resolution at 10 meters.
- Satellite time series: Up to 20 years of temporal Landsat data for six bands (R, G, B, IR, SWIR1, SWIR2), encoded as datacubes with format (years \times months \times bands).
- Climatic Data Cubes: Climatic variables from the CHELSA dataset, more precisely monthly precipitation and min, max, and mean temperature aggregated as cubes of shape (years \times months \times variables).

The training and testing data splits follow the original challenge protocol, employing a spatial block hold-out with 10×10 km grid cells. The model used corresponds to the multimodal baseline provided for the challenge and is available via [this link](#). It consists of an ensemble of two ResNet-18-based encoders for Landsat and climatic data cubes, combined with a Swin-v2-t transformer model for satellite imagery. For the scenario involving calibration on the training set, a 10% subsample of the training data is used to reduce computational and memory overhead during calibration.

4.2 Case study 2: Reef Life Survey

The second case study investigates an other DeepSDM model this time applied to the Reef Life Survey dataset on coral reef fishes ([Edgar and Stuart-Smith, 2014](#)). The dataset is composed of 27,437 underwater surveys of coastal habitats in Australia. Observations are then split randomly with a 60/20/20 percentage repartition for train/validation/test datasets, making sure that all surveys from a given location (as defined in the Reef Life Survey metadata) are in the same fold to limit spatial overlap. The original data being species abundances, it was binarized in the referenced study, resulting in a 1796-species presence-absence dataset.

The model is composed of 2 heads using respectively a time series of temperature anomaly (Degree Heating Week), and 19 rasters of instantaneous environmental conditions, 15 depicting the natural seascape, and 4 assessing the impact of human activities. Both heads rely on a ResNet-18 encoder. This case study is based on the principle described in [this article](#), with specifics of the model described ([Morand and Mouillot, 2025](#)).

4.3 Case study 3: American birds

The third case study builds upon the first scenario of the referred paper (Zipkin et al., 2023), which aims to spatially extrapolate species distributions for 27 North American bird species using data from two major citizen science programs: the Breeding Bird Survey (BBS) (Hudson et al., 2017) and eBird (Sullivan et al., 2014).

The combined dataset includes 10,383 eBird checklists (used as presence only data) and 356 BBS routes that were binarized as presence-absence records. All observations were collected in the northeastern United States during the first three weeks of June. The data were aggregated into 5×5 km grid cells, resulting in 356 spatial sites. Contrary to the original study, for the train/test split, a 10-fold spatial block cross-validation was applied to the BBS data. One fold was retained for validation and another for testing, while all eBird data were included in the training set (see Section B in Supplementary Material for the maps). Predictions from all trained models on the test fold were aggregated and evaluated against the BBS ground truth. For calibration on train, the mean probability across models trained on the respective fold was used.

5 Results

The results for each case study are summarized in (Table 2, Table 3, Table 4). For supervised methods, the parameters of each method were optimized for each column in the table, specifically to maximize the corresponding score. As mentioned before, we considered two calibration scenarios: using the training set for calibration, or using a separate validation set. The first scenario allows a more direct and fair comparison with unsupervised methods, as it does not provide additional information beyond the training data.

For each test conducted, a permutation test was performed to assess whether the mean score achieved by the proposed framework is significantly higher than that of the other methods (see Section C in the Supplementary Material).

5.1 Case Study 1

MaxExp achieves significantly higher scores than all alternatives across all scores (permutation test, $p < 0.05$), except SSE on F_1 and Jaccard, where differences are not statistically significant. Only when calibrated on the validation set, the global threshold method Th. t becomes competitive. When calibrated on training set, its performance degrades significantly.

		TARGET SCORES				
		F_1	F_2	J	TSS	
SUPERVISED METHODS	Calibrated on Train	Top K	0.319	0.446	0.203	
		Th. t	0.332	0.459	0.216	
		Th. t_f	0.305	0.395	0.198	
		R_{opti}	0.270	0.398	0.811	
	Calibrated on Validation	Top K	0.321	0.452	0.205	
		Th. t	<u>0.334</u>	<u>0.467*</u>	<u>0.218</u>	
		Th. t_f	0.311	0.410	0.200	
		R_{opti}	0.175	0.309	0.100	
UNSUPERVISED METHODS		Th. $t_{0.5}$	0.259	0.317	0.167	
		SSE (our)	0.336*	0.441	0.219*	
		MaxExp (our)	0.343	0.474	0.224	
					0.863	

Table 2: Mean scores obtained for the different methods (Table 1) applied to Case Study 1. Bold indicates the best unsupervised scores. Underlined values indicate best supervised scores. Asterisks mark results within the confidence interval of MaxExp ($p < 0.05$).

5.2 Case Study 2

In this experiment, calibration on the validation dataset substantially improved the scores of supervised methods. While MaxExp remains the top-performing unsupervised method (and also outperforms supervised methods calibrated on the training set), the globally optimized threshold method calibrated on the validation set achieves higher scores across all metrics except TSS.

		TARGET SCORES				
		F_1	F_2	J	TSS	
SUPERVISED METHODS	Calibrated on Train	Top K	0.355	0.480	0.231	0.740
		Th. t	0.360	0.479*	0.238	0.754
		Th. t_f	0.293	0.369	0.186	0.271
		R_{opti}	0.204	0.327	0.123	0.705
	Calibrated on Validation	Top K	0.357	0.487	0.230	0.740
		Th. t	<u>0.376*</u>	<u>0.507*</u>	<u>0.248*</u>	0.754
		Th. t_f	0.366	0.469	0.239	0.390
		R_{opti}	0.155	0.295	0.086	<u>0.806*</u>
UNSUPERVISED METHODS	Th. $t_{0.5}$	0.292	0.354	0.189	0.246	
	SSE (our)	0.363	0.454	0.241	0.366	
	MaxExp (our)	0.373	0.499	0.248	0.788	

Table 3: Mean scores obtained for the different methods applied to Case Study 2. Bold indicates the best unsupervised scores. Underlined values indicate best supervised scores. Asterisks mark results within the confidence interval of MaxExp ($p < 0.05$).

5.3 Case Study 3

In this third case study, MaxExp globally outperforms all other methods; only the globally optimized threshold method—whether calibrated on the training or validation set—achieves competitive performance.

		TARGET SCORES				
		F_1	F_2	J	TSS	
SUPERVISED METHODS	Calibrated on Train	Top K	0.681	0.803	0.536	
		Th. t	<u>0.707*</u>	<u>0.819*</u>	<u>0.569*</u>	
		Th. t_f	0.660	0.742	0.529	
		R_{opti}	0.652	0.790	0.510	
	Calibrated on Validation	Top K	0.675	0.795	0.536	
		Th. t	0.704*	0.819*	0.567*	
		Th. t_f	0.652	0.740	0.522	
		R_{opti}	0.645	0.778	0.503	
UNSUPERVISED METHODS		Th. $t_{0.5}$	0.645	0.722	0.513	
		SSE (our)	0.686	0.769	0.549*	
		MaxExp (our)	0.713	0.823	0.573	
					0.629	

Table 4: Mean scores obtained for the different methods applied to Case Study 3. Bold indicates the best unsupervised scores. Underlined values indicate best supervised scores. Asterisks mark results within the confidence interval of MaxExp ($p < 0.05$).

Across all three case studies, the MaxExp framework consistently improves performance across all evaluated scores among unsupervised methods and those calibrated on train set. Notably, only the test-based supervised global threshold method outperformed MaxExp on case study 2, will the latter achieve statistically significant but inferior scores in most scenarios when compared to MaxExp, using either test and train dataset for calibration.

The Set Size Expectation (SSE) method also achieves substantial performance for both the F_1 -score and the Jaccard index (J) across all of the 3 case studies. This illustrates how the number of species predicted per site—based on the sum of predicted probabilities interacts with these metrics, even though the estimated richness can be biased and highly variable in practice.

6 Discussion

6.1 Result analysis

Our study demonstrates that SDM binarization — the critical step from species probability of occurrence in a given site to presence–absence prediction — can be addressed as a decision optimization problem rather than as a heuristic approach. By adopting this change of paradigm, through the introduction of the new MaxExp framework, we show that unsupervised multispecies predictions can achieve better performances than classical methods across diverse taxa and ecosystems without additional calibration. A second insight is that

the simple Set Size Expectation (SSE) baseline is surprisingly effective, highlighting that interpretability and computational efficiency are not necessarily at the expense of predictive accuracy. Together, these findings provide ecologists with complementary tools for multi-species predictions: MaxExp as a general-purpose optimizer adapted to a large range of scores, and SSE as a lightweight, intuitive alternative for base target scores such as F_1 and Jaccard.

Our three case studies also highlight that dataset characteristics significantly condition the relative performance of binarization methods. First, for the GeoPlant dataset, which is species-rich (5,000+ taxa), spatially heterogeneous, and strongly imbalanced with a long tail of rare species (Picek et al., 2024), MaxExp clearly outperforms other methods across all scores, highlighting its relevance for high-dimensional and imbalanced conditions, which are common in ecology. SSE also performs well for F_1 and Jaccard, reflecting the close alignment of predicted and observed richness with these scores in highly diverse communities.

In contrast, for the Reef Life Survey fish dataset (Edgar and Stuart-Smith, 2014), which presents a smaller number of sites but still a high number of species. the supervised thresholding methods calibrated on a validation set perform better than on GeoPlant, in some cases rivaling with MaxExp. This suggests that in datasets with strong distribution shifts between train and test datasets, the use of supervised calibration similar to the test sets can partially compensate for miscalibrated probability estimates.

Alternatively, one could have calibrated the predictive models themselves on the validation set and then applied MaxExp to the resulting probabilities. This would likely have yielded higher performance than the supervised methods, as these methods already achieve results comparable to MaxExp in its unsupervised form.

Finally, for the North American bird dataset including relatively few species and sites, with data aggregated from standardized monitoring (BBS) (Hudson et al., 2017) and citizen science (eBird) (Sullivan et al., 2014), MaxExp outperforms reference methods for every scores. The performance gap between thresholding approaches is nonetheless smaller than in the previous case studies. We hypothesize that the limited number of species, restricted geographical region, and narrow sampling timeframe produced a dataset with low variance, reducing the advantage of unsupervised methods. This hypothesis is supported by a table of scores higher and far more homogenous than for previous cases, and by a model with the best calibration curve on test of the three cases, despite being the simplest (Figure 4, Supplementary Material). The smaller taxonomic and spatial scope, combined with better-calibrated probabilities results in the global threshold method performing competitively, and differences between MaxExp, SSE, and calibration-based methods were less pronounced.

6.2 Metric choice

Another important consideration, as emphasized in the introduction (see Figure 2), is that the selection of a specific evaluation metric inherently determines the nature of the resulting predictions. The optimization process, either unsupervised or related to a calibration step, is metric-dependent, and different target scores can lead to substantially divergent spatial

and statistical patterns of predicted species prevalence (Hellegers et al., 2025) or biodiversity composition. Each evaluation metric embodies a distinct conceptualization of predictive accuracy—prioritizing, for example, the detection of rare species, the minimization of false positives, or the achievement of realistic overall prevalence estimates.

Within this framework, the F_β family of scores provides a clear illustration of how varying the parameter β allows one to adjust the relative importance of false negatives and false positives. Although the functional relationship between β and its influence on the optimized prediction thresholds is not analytically straightforward, empirical evidence indicate that higher values of β tend to produce larger predicted species sets (Figure 2). This reflects an increased tolerance for false positives while reducing the number of false negatives.

While the balanced F_1 -score remains the predominant choice in the literature, adopting higher β values may be particularly relevant in ecological contexts where false negatives are more detrimental than false positives. Such situations include, for example, the assessment of potential favorable habitat or refuges for rare or endangered species (Pichot et al., 2025, Semper-Pascual et al., 2023, or scenarios where repeated non-detections compromise confidence in absence predictions.

6.3 Limitations and Perspectives

The present study focused on sample-averaged metrics, i.e., metrics that measure model performance over species assemblages per site. However, MaxExp can also be applied to macro-averaged metrics, i.e., metrics that measure model performance over mean prevalence per species, then averaged across species. This extension is partially exposed in Section E of the Supplementary Material. However, if theoretical results are invariant to the transposition of the problem, our tests conclude that the robustness to concrete cases of the MaxExp framework may not be translated to the macro-averaged score optimization. If MaxExp still leads to performance improvement in several experiments, this difference is not anymore systematic and the results vary from case studies and from chosen scores. The scores being significantly lower than their sample-average equivalent, the error in probability estimates for some species impact more greatly macro-average scores. Besides, if Top K method for macro-averaged scores is not adapted due to strong species prevalence, species-related threshold method Th. t_s can in this case be computed, and can seemingly lead to improved performances for validation-based calibration.

A second limitation of MaxExp lies in its implicit assumption of species independence, which overlooks ecological interactions such as facilitation or competition (Steen et al., 2014). In this respect, MaxExp aligns with most binarization methods found in the literature. However, recent studies have sought to move beyond this assumption, for instance with the threshold classifier proposed by (Dorm et al., 2024). Addressing these challenges — e.g., by integrating species co-occurrence models, trait-based approaches, or new evaluation scores — represents an important direction for future research.

Regarding methodological perspectives, future work could explore the comparison with

end-to-end learning of score-aware predictors (Calabrese et al., 2014), where the optimization of evaluation criteria is embedded directly into the training phase of the models rather than in a post hoc binarization. Finally, the explicit link between decision rules and evaluation scores invites a broader assessment of how the choice of scores aligns with predictive tasks, highlighting the importance of a thoughtful evaluation metric selection and opening the way to score design tailored to conservation priorities, notably emphasizing endangered or rare species (Mouillot et al., 2024).

In conclusion, two main messages emerge. First, MaxExp provides a flexible, unsupervised optimization framework that improves presence-absence predictions for most commonly used evaluation scores of species assemblage predictions. SSE additionally offers a simple and efficient alternative which, while not always matching MaxExp, performs competitively under two of the four scores considered. Together, these approaches reframe binarization not as a heuristic compromise but as a transparent and reproducible decision process that can be explicitly aligned with ecological objectives of decision-making (Guisan et al., 2013, Kass et al., 2024).

7 Acknowledgements

The research described in this paper was funded by the European Commission through the MAMBO project (grant agreement 101060639) and the GUARDEN project (grant agreement 101060693). The authors would also want to thanks the CNRS GDR OMER for its support and resources.

8 Conflict of Interest

The authors declare no conflicts of interest.

References

Allouche, O., Tsoar, A., & Kadmon, R. (2006). Assessing the accuracy of species distribution models: Prevalence, kappa and the true skill statistic (TSS). *Journal of Applied Ecology*, 43(6), 1223–1232. <https://doi.org/10.1111/j.1365-2664.2006.01214.x>

Angelopoulos, A. N., & Bates, S. (2022, December 7). *A Gentle Introduction to Conformal Prediction and Distribution-Free Uncertainty Quantification*. arXiv: 2107.07511 [cs]. <https://doi.org/10.48550/arXiv.2107.07511>

Araújo, M. B., Thuiller, W., & Pearson, R. G. (2006). Climate warming and the decline of amphibians and reptiles in europe. *Journal of Biogeography*, 33(10), 1712–1728. <https://doi.org/https://doi.org/10.1111/j.1365-2699.2006.01482.x>

Calabrese, J. M., Certain, G., Kraan, C., & Dormann, C. F. (2014). Stacking species distribution models and adjusting bias by linking them to macroecological models. *Global Ecology and Biogeography*, 23(1), 99–112. <https://doi.org/10.1111/geb.12102>

Chambert, T., Miller, D. A. W., & Nichols, J. D. (2015). Modeling false positive detections in species occurrence data under different study designs. *Ecology*, 96(2), 332–339. <https://doi.org/https://doi.org/10.1890/14-1507.1>

Chollet Ramampiandra, E., Scheidegger, A., Wydler, J., & Schuwirth, N. (2023). A comparison of machine learning and statistical species distribution models: Quantifying overfitting supports model interpretation. *Ecological Modelling*, 481, 110353. <https://doi.org/10.1016/j.ecolmodel.2023.110353>

Deneu, B., Servajean, M., Bonnet, P., Botella, C., Munoz, F., & Joly, A. (2021). Convolutional neural networks improve species distribution modelling by capturing the spatial structure of the environment. *PLoS Computational Biology*, 17(4), e1008856. <https://doi.org/10.1371/journal.pcbi.1008856>

Dirzo, R., Young, H. S., Galetti, M., Ceballos, G., Isaac, N. J. B., & Collen, B. (2014). Defaunation in the anthropocene. *Science*, 345(6195), 401–406. <https://doi.org/10.1126/science.1251817>

Dorm, F., Lange, C., Loarie, S., & Aodha, O. M. (2024, August 28). *Generating Binary Species Range Maps*. arXiv: 2408.15956 [q-bio]. <https://doi.org/10.48550/arXiv.2408.15956>

Edgar, G., & Stuart-Smith, R. (2014). Systematic global assessment of reef fish communities by the reef life survey program. *Scientific data*, 1, 140007. <https://doi.org/10.1038/sdata.2014.7>

Guisan, A., & Rahbek, C. (2011). SESAM – a new framework integrating macroecological and species distribution models for predicting spatio-temporal patterns of species assemblages. *Journal of Biogeography*, 38(8), 1433–1444. <https://doi.org/10.1111/j.1365-2699.2011.02550.x>

Guisan, A., & Thuiller, W. (2005). Predicting species distribution: Offering more than simple habitat models. *Ecology Letters*, 8(9), 993–1009. <https://doi.org/10.1111/j.1461-0248.2005.00792.x>

Guisan, A., Tingley, R., Baumgartner, J. B., Naujokaitis-Lewis, I., Sutcliffe, P. R., Tulloch, A. I. T., Regan, T. J., Brotons, L., McDonald-Madden, E., Mantyka-Pringle, C., Martin, T. G., Rhodes, J. R., Maggini, R., Setterfield, S. A., Elith, J., Schwartz, M. W., Wintle, B. A., Broennimann, O., Austin, M., ... Buckley, Y. M. (2013). Predicting species distributions for conservation decisions. *Ecology Letters*, 16(12), 1424–1435. <https://doi.org/10.1111/ele.12189>

Hellegers, M., van Hinsberg, A., Lenoir, J., Dengler, J., Huijbregts, M. A. J., & Schipper, A. M. (2025). Multiple Threshold-Selection Methods Are Needed to Binarise Species Distribution Model Predictions. *Diversity and Distributions*, 31(4), e70019. <https://doi.org/10.1111/ddi.70019>

Hudson, M.-A. R., Francis, C. M., Campbell, K. J., Downes, C. M., Smith, A. C., & Pardieck, K. L. (2017). The role of the North American Breeding Bird Survey in conservation. *The Condor: Ornithological Applications*, 119(3), 526–545. <https://doi.org/10.1650/CONDOR-17-62.1>

Jiménez-Valverde, A., & Lobo, J. M. (2007). Threshold criteria for conversion of probability of species presence to either-or presence-absence. *Acta Oecologica*, 31(3), 361–369. <https://doi.org/https://doi.org/10.1016/j.actao.2007.02.001>

Kass, J. M., Fukaya, K., Thuiller, W., & Mori, A. S. (2024). Biodiversity modeling advances will improve predictions of nature's contributions to people. *Trends in Ecology & Evolution*, 39(4), 338–348. <https://doi.org/https://doi.org/10.1016/j.tree.2023.10.011>

Laurance, W., Nascimento, H., Laurance, S., Andrade, A., Ewers, R., Harms, K., Luizão, R., & Ribeiro, J. (2007). Habitat Fragmentation, Variable Edge Effects, and the Landscape-Divergence Hypothesis. *PloS one*, 2, e1017. <https://doi.org/10.1371/journal.pone.0001017>

Legendre, P., & Legendre, L. (2012). *Numerical ecology*. Elsevier.

Leroy, B., Delsol, R., Hugueny, B., Meynard, C. N., Barhoumi, C., Barbet-Massin, M., & Bellard, C. (2018). Without quality presence-absence data, discrimination metrics such as TSS can be misleading measures of model performance. *Journal of Biogeography*, 45(9), 1994–2002. Retrieved May 16, 2025, from <https://www.jstor.org/stable/26629096>

Li, W., & Guo, Q. (2013). How to assess the prediction accuracy of species presence-absence models without absence data? *Ecography*, 36(7), 788–799. <https://doi.org/10.1111/j.1600-0587.2013.07585.x>

Luoto, M., Heikkinen, R. K., Pöyry, J., & Saarinen, K. (2006). Determinants of the biogeographical distribution of butterflies in boreal regions. *Journal of Biogeography*, 33(10), 1764–1778. Retrieved October 1, 2025, from <http://www.jstor.org/stable/3838515>

Morand, G., & Mouillot, D. (2025). A multi-modal resnet model to predict coastal fish occurrences using a seascape approach. *bioRxiv*. <https://doi.org/10.1101/2025.10.29.682812>

Mouillot, D., Velez, L., Albouy, C., Casajus, N., Claudet, J., Delbar, V., Devillers, R., Letessier, T. B., Loiseau, N., Manel, S., Mannocci, L., Meeuwig, J., Mouquet, N., Nuno, A., O'Connor, L., Parravicini, V., Renaud, J., Seguin, R., Troussellier, M., & Thuiller, W. (2024). The socioeconomic and environmental niche of protected areas reveals global conservation gaps and opportunities. *Nature Communications*, 15(1), 9007. <https://doi.org/10.1038/s41467-024-53241-1>

Nan, Y., Chai, K. M., Lee, W. S., & Chieu, H. L. (2012, June 18). *Optimizing F-measure: A Tale of Two Approaches*. arXiv: 1206.4625 [cs]. <https://doi.org/10.48550/arXiv.1206.4625>

Nenzén, H. K., & Araújo, M. B. (2011). Choice of threshold alters projections of species range shifts under climate change. *Ecological Modelling*, 222(18), 3346–3354. <https://doi.org/10.1016/j.ecolmodel.2011.07.011>

Petitpierre, B., Broennimann, O., Kueffer, C., Daehler, C., & Guisan, A. (2017). Selecting predictors to maximize the transferability of species distribution models: Lessons from cross-continental plant invasions. *Global Ecology and Biogeography*, 26(3), 275–287. <https://doi.org/10.1111/geb.12530>

Picek, L., Botella, C., Servajean, M., Leblanc, C., Palard, R., Larcher, T., Deneu, B., Marcos, D., Estopinan, J., Bonnet, P., & Joly, A. (2024). Overview of GeoLifeCLEF 2024: Species Composition Prediction with High Spatial Resolution at Continental Scale using Remote Sensing. *3740*(186), 1966. Retrieved December 11, 2024, from <https://hal.inrae.fr/hal-04720817>

Pichot, F., Manel, S., Velez, L., Juhel, J.-B., Ballesta, L., Boissery, P., Bruno, M., Cancemi, M., Holon, F., Riutort, J.-J., Schultz, M., Tomasi, N., Valentini, A., Adam, O., Deter,

J., & Mouillot, D. (2025). Mesophotic protected habitats as refugia for the most at-risk elasmobranch species. *Biological Conservation*, 310, 111371. <https://doi.org/https://doi.org/10.1016/j.biocon.2025.111371>

Randin, C. F., Dirnböck, T., Dullinger, S., Zimmermann, N. E., Zappa, M., & Guisan, A. (2006). Are niche-based species distribution models transferable in space? *Journal of Biogeography*, 33(10), 1689–1703. <https://doi.org/10.1111/j.1365-2699.2006.01466.x>

Semper-Pascual, A., Sheil, D., Beaudrot, L., Dupont, P., Dey, S., Ahumada, J., Akampurira, E., Bitariho, R., Espinosa, S., Jansen, P. A., Lima, M. G. M., Martin, E. H., Mugerwa, B., Rovero, F., Santos, F., Uzabaho, E., & Bischof, R. (2023). Occurrence dynamics of mammals in protected tropical forests respond to human presence and activities. *Nature Ecology & Evolution*, 7(7), 1092–1103. <https://doi.org/10.1038/s41559-023-02060-6>

Steen, D. A., McClure, C. J. W., Brock, J. C., Craig Rudolph, D., Pierce, J. B., Lee, J. R., Jeffrey Humphries, W., Gregory, B. B., Sutton, W. B., Smith, L. L., Baxley, D. L., Stevenson, D. J., & Guyer, C. (2014). Snake co-occurrence patterns are best explained by habitat and hypothesized effects of interspecific interactions. *Journal of Animal Ecology*, 83(1), 286–295. <https://doi.org/https://doi.org/10.1111/1365-2656.12121>

Sullivan, B. L., Aycrigg, J. L., Barry, J. H., Bonney, R. E., Bruns, N., Cooper, C. B., Damoulas, T., Dhondt, A. A., Dietterich, T., Farnsworth, A., Fink, D., Fitzpatrick, J. W., Fredericks, T., Gerbracht, J., Gomes, C., Hochachka, W. M., Iliff, M. J., Lagoze, C., La Sorte, F. A., . . . Kelling, S. (2014). The eBird enterprise: An integrated approach to development and application of citizen science. *Biological Conservation*, 169, 31–40. <https://doi.org/10.1016/j.biocon.2013.11.003>

Wilkinson, D. P., Golding, N., Guillera-Arroita, G., Tingley, R., & McCarthy, M. A. (2021). Defining and evaluating predictions of joint species distribution models. *Methods in Ecology and Evolution*, 12(3), 394–404. <https://doi.org/https://doi.org/10.1111/2041-210X.13518>

Zipkin, E. F., Doser, J. W., Davis, C. L., Leuenberger, W., Ayebare, S., & Davis, K. L. (2023). Integrated community models: A framework combining multispecies data sources to estimate the status, trends and dynamics of biodiversity. *Journal of Animal Ecology*, 92(12), 2248–2262. <https://doi.org/10.1111/1365-2656.14012>

Zizka, A., Azevedo, J., Leme, E., Neves, B., da Costa, A. F., Caceres, D., & Zizka, G. (2020). Biogeography and conservation status of the pineapple family (Bromeliaceae). *Diversity and Distributions*, 26(2), 183–195. <https://doi.org/10.1111/ddi.13004>

Zurell, D., Zimmermann, N. E., Gross, H., Baltensweiler, A., Sattler, T., & Wüest, R. O. (2020). Testing species assemblage predictions from stacked and joint species distribution models. *Journal of Biogeography*, 47(1), 101–113. <https://doi.org/10.1111/jbi.13608>

¹ **1 Supplementary Material**

² **A MaxExp Algorithm**

³ The MaxExp algorithm. No assumption about the score U is presumed besides **A1** and
⁴ **A2**. Consequently the resolution is in $\mathcal{O}(N^3)$ complexity, where N denotes the number of
⁵ species of interest. It takes in input the estimated probability vector $\hat{\eta}$ and the score U and
⁶ return the set of predicted species. Assumption **A1** and **A2** allows us to stop at the first
⁷ expected score maximum, diminishing greatly in average the number of expected score $S(K)$
⁸ to compute.

Algorithm 1: MaxExp($\hat{\eta}$, U)

Input: $\hat{\eta}$, U

Output: K^{th} most probable species

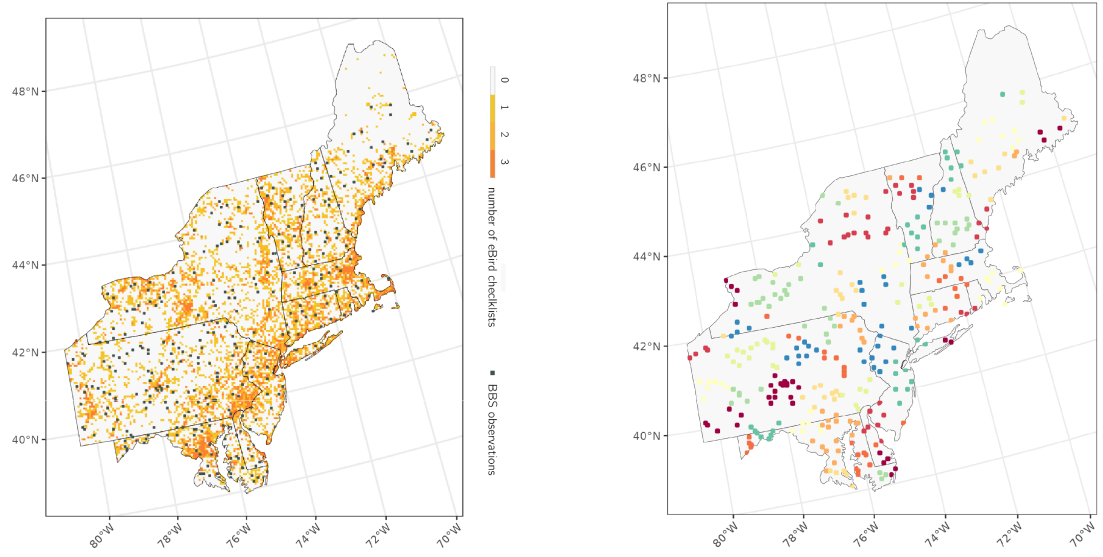
1. Compute the probability matrices

```
 $P, P' \leftarrow O_{N+1}, O_{N+1}$ 
 $\eta \leftarrow \text{sort}(\hat{\eta}, \text{'decreasing'})$ 
 $P_{1,1}, P'_{1,1} \leftarrow 1, 1$ 
for  $i \in \llbracket 1, N \rrbracket$  do
   $P_{i+1,0} \leftarrow (1 - \eta_i)P_{i,0}$ 
  for  $j \in \llbracket 1, i+1 \rrbracket$  do
     $P_{i+1,j+1} \leftarrow \eta_i P_{i,j} + (1 - \eta_i)P_{i,j+1}$ 
  end
end
for  $i \in \llbracket 1, N \rrbracket$  do
   $P'_{i+1,0} \leftarrow (1 - \eta_{N-i+1})P'_{i,0}$ 
  for  $j \in \llbracket 1, i+1 \rrbracket$  do
     $P'_{i+1,j+1} \leftarrow \eta_{N-i+1}P'_{i,j} + (1 - \eta_{N-i+1})P'_{i,j+1}$ 
  end
end
```

2. Compute expected score $S(K)$ with K running from 1 to first maximum

```
 $S^*, S, K^*, K \leftarrow -\infty, -\infty, 0, 0$ 
while  $K \leq N$  and  $S = S^*$  do
   $S \leftarrow 0$ 
  for  $i \in \llbracket 1, K+1 \rrbracket$  do
    for  $j \in \llbracket 1, N-K+1 \rrbracket$  do
      Increment  $S(K)$  along  $U(\text{TP}, \text{FP}, \text{FN}, \text{TN})$ 
       $S \leftarrow S + P_{K,i} S_{N-K,j} \times U(i, K-i, j, N-K-j)$ 
    end
  end
  if  $S > S^*$  then
     $S^*, K^* \leftarrow S, K$ 
  end
end
return  $K^{\text{th}}$  most probable species
```

10 **B Maps American Birds**



(a) Density of Bird checklists and location of the BBS routes.

(b) Folds from BBS checklists, determined by a group of dots (representing sites) of the same color

Figure 1: Distribution of sites and observations used in the third case study.

11 **C Permutation test p-values**

		TARGET SCORES			
		F_1	F_2	J	TSS
SUPERVISED METHODS	Calibrated on Train	Top K	$< 10^{-4}$	$< 10^{-4}$	$< 10^{-4}$
		Th. t	10^{-3}	10^{-3}	0.01
		Th. t_f	$< 10^{-4}$	$< 10^{-4}$	$< 10^{-4}$
		R_{opti}	$< 10^{-4}$	$< 10^{-4}$	$< 10^{-4}$
	Calibrated on Validation	Top K	$< 10^{-4}$	$< 10^{-4}$	$< 10^{-4}$
		Th. t	0.02	<u>0.09</u>	0.05
		Th. t_f	$< 10^{-4}$	$< 10^{-4}$	$< 10^{-4}$
		R_{opti}	$< 10^{-4}$	$< 10^{-4}$	$< 10^{-4}$
UNSUPERVISED METHODS		Th. $t_{0.5}$	$< 10^{-4}$	$< 10^{-4}$	10^{-4}
		SSE (our)	<u>0.06</u>	$< 10^{-4}$	0.10

Table 1: p-values from permutation test of scores S ($H_1 : \mathbb{E}[S_{\text{MaxExp}}] > \mathbb{E}[S]$, $n_{\text{per}} = 9999$). For p-values < 0.01 , only order of magnitude is shown. Cases where the score is statistically significant are underlined.

		TARGET SCORES			
		F_1	F_2	J	TSS
SUPERVISED METHODS	Calibrated on Train	Top K	$< 10^{-4}$	$< 10^{-4}$	$< 10^{-4}$
		Th. t	10^{-3}	$< 10^{-4}$	10^{-3}
		Th. t_f	$< 10^{-4}$	$< 10^{-4}$	$< 10^{-4}$
		R_{opti}	$< 10^{-4}$	$< 10^{-4}$	$< 10^{-4}$
	Calibrated on Validation	Top K	$< 10^{-4}$	10^{-3}	$< 10^{-4}$
		Th. t	0.7	0.96	0.55
		Th. t_f	0.05	$< 10^{-4}$	10^{-3}
		R_{opti}	$< 10^{-4}$	$< 10^{-4}$	$< 10^{-4}$
UNSUPERVISED METHODS		Th. $t_{0.5}$	$< 10^{-4}$	$< 10^{-4}$	$< 10^{-4}$
		SSE (our)	0.01	$< 10^{-4}$	0.04

Table 2: p-values from permutation test for Case Study 2. Format and significance markers as in Table 1.

		TARGET SCORES				
		F_1	F_2	J	TSS	
SUPERVISED METHODS	Calibrated on Train	Top K	0.01	0.03	10^{-2}	
		Th. t	<u>0.34</u>	<u>0.36</u>	<u>0.38</u>	
		Th. t_f	10^{-3}	$< 10^{-4}$	10^{-2}	
		R_{opti}	$< 10^{-4}$	10^{-3}	10^{-4}	
	Calibrated on Validation	Top K	10^{-3}	10^{-3}	10^{-2}	
		Th. t	<u>0.27</u>	<u>0.33</u>	<u>0.36</u>	
		Th. t_f	10^{-4}	$< 10^{-4}$	10^{-3}	
		R_{opti}	$< 10^{-4}$	10^{-4}	$< 10^{-4}$	
UNSUPERVISED METHODS		Th. $t_{0.5}$	$< 10^{-4}$	$< 10^{-4}$	10^{-4}	
		SSE (our)	0.03	$< 10^{-4}$	<u>0.06</u>	
					$< 10^{-4}$	

Table 3: p-values from permutation test for Case Study 3. Format and significance markers as in Table 1.

₁₂ **D Calibration curves**

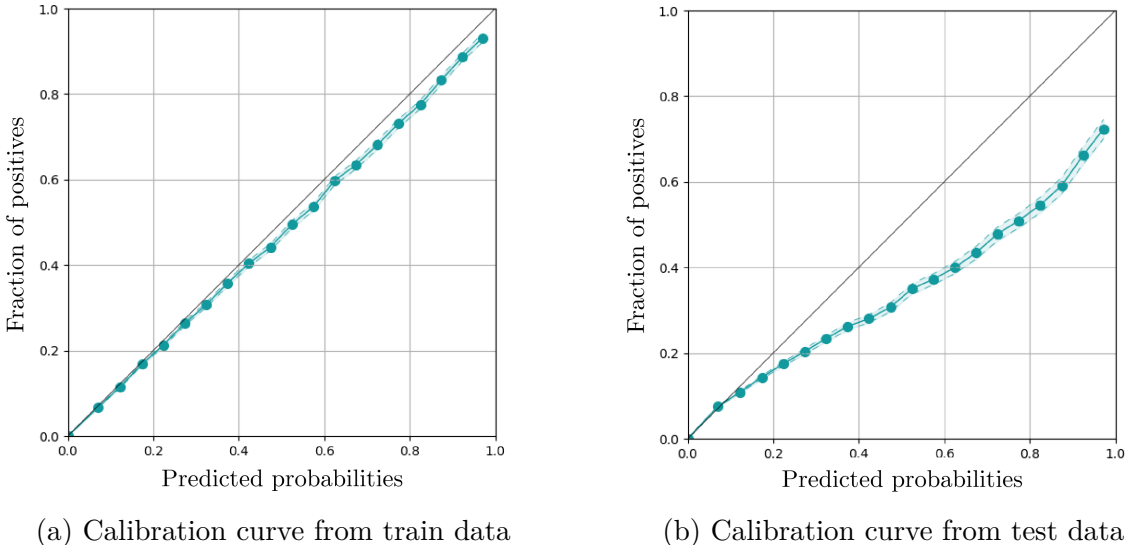
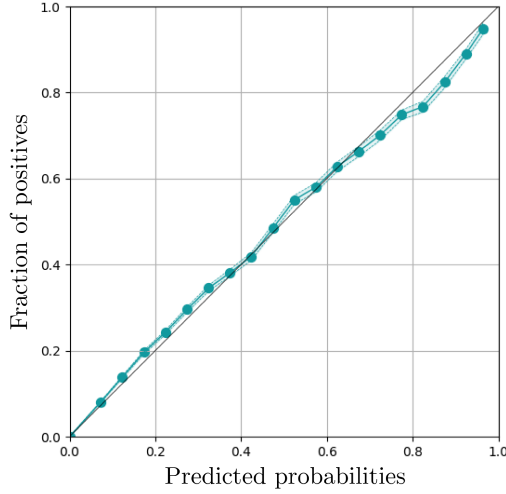
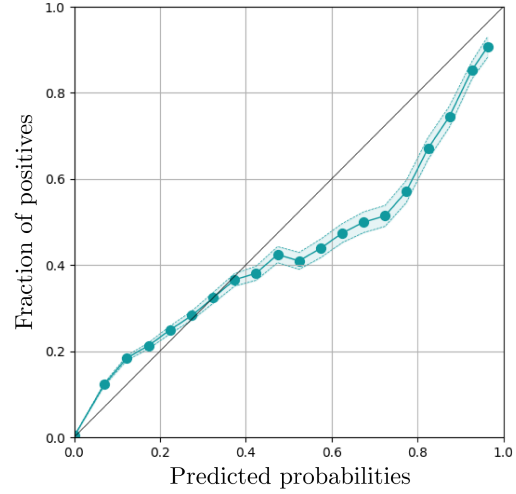


Figure 2: Calibration curves from the model and data in the first study. The predicted probabilities across all sites and species are placed in bins, and the fraction of presences are calculated from the related observations. The blue zone corresponds to an estimation of a $\pm 2\sigma$ interval. We can clearly observe over-predictions of the model for the test set, which can affect the viability of MaxExp to find the expected optimum.

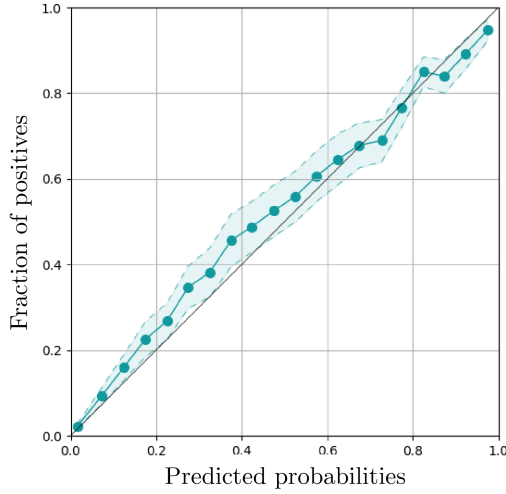


(a) Calibration curve from train data

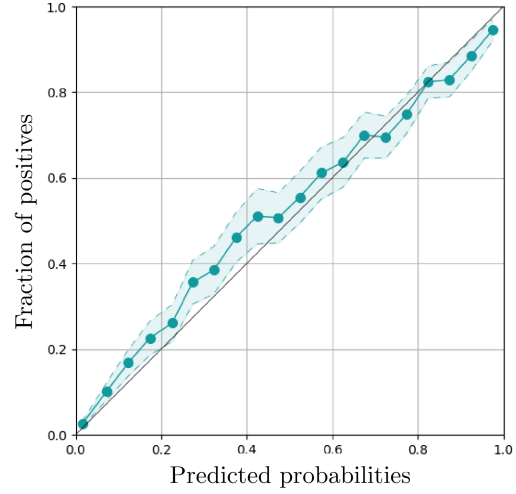


(b) Calibration curve from test data

Figure 3: Calibration curves from the model and data in the second study. The predicted probabilities across all sites and species are placed in bins, and the fraction of presences are calculated from the related observations. The blue zone corresponds to an estimation of a $\pm 2\sigma$ interval.



(a) Calibration curve from train data



(b) Calibration curve from test data

Figure 4: Calibration curves from the model and data in the third study. The predicted probabilities across all sites and species are placed in bins, and the fraction of presences are calculated from the related observations. The blue zone corresponds to an estimation of a $\pm 2\sigma$ interval.

¹³ **E Macro-averaged scores**

		TARGET SCORES			
		F_1	F_2	J	TSS
SUPERVISED METHODS	Calibrated on Train	Th. t	0.087	0.132	0.057
		Th. t_s	0.086	0.128	0.056
		Th. t_f	0.076	0.101	0.049
		R_{opti}	0.071	0.110	0.198
	Calibrated on Validation	Th. t	0.089	0.138	0.057
		Th. t_s	<u>0.092</u>	<u>0.140</u>	<u>0.058</u>
		Th. t_f	0.075	0.103	0.047
		R_{opti}	0.070	0.106	0.201
UNSUPERVISED METHODS	Th. $t_{0.5}$		0.054	0.067	0.036
	SSE (our)		0.088	0.118	0.057
	MaxExp (our)		0.103	0.151	0.066
		0.379			

Table 4: Mean of the macro-averaged scores S_m obtained for the different methods applied to Case Study 1. The best scores obtained on unsupervised methods are in bold while those obtained on supervised methods are underlined.

		TARGET SCORES				
		F_1	F_2	J	TSS	
SUPERVISED METHODS	Calibrated on Train	Th. t	0.072	0.119	0.043	0.206
		Th. t_s	0.052	0.082	0.033	0.181
		Th. t_f	0.041	0.053	0.026	0.034
		R_{opti}	0.040	0.059	0.025	0.196
	Calibrated on Validation	Th. t	0.083	0.133	0.051	0.206
		Th. t_s	<u>0.089</u>	0.136	<u>0.056</u>	0.167
		Th. t_f	0.074	0.100	0.046	0.071
		R_{opti}	0.086	<u>0.138</u>	0.055	<u>0.249</u>
UNSUPERVISED METHODS	Th. $t_{0.5}$		0.026	0.031	0.017	0.019
	SSE (our)		0.054	0.071	0.033	0.044
	MaxExp (our)		0.073	0.116	0.045	0.314

Table 5: Mean of the macro-averaged scores S_m obtained for the different methods applied to Case Study 2. The best scores obtained on unsupervised methods are in bold while those obtained on supervised methods are underlined.

		TARGET SCORES				
		F_1	F_2	J	TSS	
SUPERVISED METHODS	Calibrated on Train	Th. t	0.645	0.782	0.507	0.412
		Th. t_s	<u>0.673</u>	<u>0.801</u>	<u>0.531</u>	<u>0.516</u>
		Th. t_f	0.641	0.738	0.493	0.413
		R_{opti}	0.641	0.769	0.496	0.481
	Calibrated on Validation	Th. t	0.638	0.786	0.509	0.415
		Th. t_s	0.652	0.785	0.507	0.471
		Th. t_f	0.654	0.759	0.504	0.442
		R_{opti}	0.637	0.777	0.492	0.435
UNSUPERVISED METHODS	Th. $t_{0.5}$		0.593	0.670	0.456	0.366
	SSE (our)		0.638	0.737	0.485	0.446
	MaxExp (our)		0.663	0.785	0.515	0.492

Table 6: Mean of the macro-averaged scores S_m obtained for the different methods applied to Case Study 3. The best scores obtained on unsupervised methods are in bold while those obtained on supervised methods are underlined.